Antibodies and staining

Flow cytometry was performed with a FACSCalibur (Becton Dickinson) as described[8,23]. Phycoerythrin (PE)- or allophycocyanin (APC)-labelled anti-CD4 (L3T4), anti-CD8 (53-6.7) and anti-B220 (RA3-6B2), PE- or fluorescein isothiocyanate (FITC)-labelled anti-TCRβ (H57-597) and anti-IgM (M41), FITC-labelled anti-TCRγδ (GL3) and PE-labelled anti-H-2K^b (AF6-88.5) antibodies were purchased from PharMingen. Cell-cycle analysis was done by flow cytometry as described[9].

PCR analysis

The PCR conditions and primers for amplifying D_HJ_H rearrangements were as described[6,24]. $D_{\beta}2J_{\beta}2$ rearrangements of the *TCRβ* locus were determined, using known PCR conditions and primers recognizing sequences 5′ of the *Dβ2.1* element or 3′ of the *Jβ2.7* element[18]. The expression of the λ*5*, *VpreB*, *pTα* and *β-actin* genes was determined by PCR with reverse transcription (RT-PCR), using published primers and conditions[25,26].

GFP analysis in thymus cryosections

To preserve GFP expression, thymi were fixed overnight in 4% paraformaldehyde at 4 °C. Fixed thymi were embedded in Tissue-Tek OCT compound, and 6 μm-thick cryosections were prepared. After mounting in PBS containing 50% glycerol, sections were analysed on a fluorescence microscope (Zeiss Axiophot) equipped with a CCD camera (Photometrics).

Received 12 May; accepted 9 August 1999.

1. Bain, G. *et al.* E2A proteins are required for proper B cell development and initiation of immunoglobulin gene rearrangements. *Cell* **79,** 885–892 (1994).
2. Zhuang, Y., Soriano, P. & Weintraub, H. The helix-loop-helix gene E2A is required for B cells formation. *Cell* **79,** 875–884 (1994).
3. Lin, H. & Grosschedl, R. Failure of B-cell differentiation in mice lacking the transcription factor EBF. *Nature* **376,** 263–267 (1995).
4. Melchers, F. & Rolink, A. in *Fundamental Immunology* (ed. Paul, W. E.) 183–224 (Lippincott-Raven, Philadelphia, 1999).
5. Urbánek, P., Wang, Z.-Q., Fetka, I., Wagner, E. F. & Busslinger, M. Complete block of early B cell differentiation and altered patterning of the posterior midbrain in mice lacking Pax5/BSAP. *Cell* **79,** 901–912 (1994).
6. Nutt, S. L., Urbánek, P., Rolink, A. & Busslinger, M. Essential functions of Pax5 (BSAP) in pro-B cell development: difference between fetal and adult B lymphopoiesis and reduced *V*-to-*DJ* recombination at the *IgH* locus. *Genes Dev.* **11,** 476–491 (1997).
7. Nutt, S. L., Morrison, A. M., Dörfler, P., Rolink, A. & Busslinger, M. Identification of BSAP (Pax5) target genes in early B-cell development by loss- and gain-of-function experiments. *EMBO J.* **17,** 2319–2333 (1998).
8. Rolink, A., Kudo, A., Karasuyama, H., Kikuchi, Y. & Melchers, F. Long-term proliferating early pre B cell lines and clones with the potential to develop to surface-Ig positive, mitogen-reactive B cells *in vitro* and *in vivo*. *EMBO J.* **10,** 327–336 (1991).
9. Rolink, A., Grawunder, U., Winkler, T. H., Karasuyama, H. & Melchers, F. IL-2 receptor α chain (CD25, TAC) expression defines a crucial stage in pre-B cell development. *Int. Immunol.* **6,** 1257–1264 (1994).
10. Reininger, L., Radaszkiewicz, T., Kosco, M., Melchers, F. & Rolink, A. G. Development of autoimmune disease in SCID mice populated with long-term *in vitro* proliferating (NZB × NZW)F1 pre-B cells. *J. Exp. Med.* **176,** 1343–1353 (1992).
11. Reininger, L. *et al.* Intrinsic B cell defects in NZB and NZW mice contribute to systemic lupus erythematosus in (NZB × NZW)F1 mice. *J. Exp. Med.* **184,** 853–861 (1996).
12. Nutt, S. L., Heavey, B., Rolink, A. G. & Busslinger, M. Commitment to the B-lymphoid lineage depends on the transcription factor Pax5. *Nature* **401,** 556–562 (1999).
13. Fehling, H. J., Krotkova, A., Saint-Ruf, C. & von Boehmer, H. Crucial role of the pre-T-cell receptor-α gene in development of α/β but not γ/δ T cells. *Nature* **375,** 795–798 (1995).
14. Ceredig, R. & Schreyer, M. Immunohistochemical localization of host and donor-derived cells in the regenerating thymus of radiation bone marrow chimeras. *Thymus* **6,** 15–26 (1984).
15. Born, W., White, J., Kappler, J. & Marrack, P. Rearrangement of IgH genes in normal thymocyte development. *J. Immunol.* **140,** 3228–3232 (1988).
16. Wang, H., Diamond, R. A. & Rothenberg, E. V. Cross-lineage expression of Ig-β (B29) in thymocytes: positive and negative gene regulation to establish T cell identity. *Proc. Natl Acad. Sci. USA* **95,** 6831–6836 (1998).
17. Kondo, M., Weissman, I. L. & Akashi, K. Identification of clonogenic common lymphoid progenitors in mouse bone marrow. *Cell* **91,** 661–672 (1997).
18. Rodewald, H.-R., Kretzschmar, K., Takeda, S., Hohl, C. & Dessing, M. Identification of pro-thymocytes in murine fetal blood: T lineage commitment can precede thymus colonisation. *EMBO J.* **13,** 4229–4240 (1994).
19. Grigoriadis, A. *et al.* Fos: a key regulator of osteoclast-macrophage lineage determination and bone remodeling. *Science* **266,** 443–448 (1994).
20. Shinkai, Y. *et al.* RAG-2-deficient mice lack mature lymphocytes owing to inability to initiate V(D)J rearrangement. *Cell* **68,** 855–867 (1992).
21. Markowitz, D., Goff, S. & Bank, A. A safe packaging line for gene transfer: separating viral genes on two different plasmids. *J. Virol.* **62,** 1120–1124 (1988).
22. Backstrom, B. T. *et al.* A motif within the T cell receptor α chain constant region connecting peptide domain controls antigen responsiveness. *Immunity* **5,** 437–447 (1996).
23. Rolink, A., Grawunder, U., Haasner, D., Strasser, A. & Melchers, F. Immature surface Ig$^+$ B cells can continue to rearrange κ and λ L chain gene loci. *J. Exp. Med.* **178,** 1263–1270 (1993).
24. Gu, H., Kitamura, D. & Rajewsky, K. B cell development regulated by gene rearrangement: arrest of maturation by membrane-bound Dμ protein and selection of D_H element reading frames. *Cell* **65,** 47–54 (1991).
25. Grawunder, U., Haasner, D., Melchers, F. & Rolink, A. Rearrangement and expression of κ light chain genes can occur without μ heavy chain expression during differentiation of pre-B cells. *Int. Immunol.* **5,** 1609–1618 (1993).
26. Bruno, L., Rocha, B., Rolink, A., von Boehmer, H. & Rodewald, H. R. Intra- and extra-thymic expression of the pre-T cell receptor α gene. *Eur. J. Immunol.* **25,** 1877–1882 (1995).

Acknowledgements

We thank J. Andersson, K. Karjalainen and E. Palmer for critical reading of the manuscript; A. Groenewegen, N. Straube, M. Dessing and A. Pickert for technical assistance; E. Wagner for animal husbandry; and T. Winkler for the GFP retrovirus. This work was supported by the Basel Institute for Immunology, the I.M.P. Vienna and a grant from the Austrian Industrial Research Promotion Fund. The Basel Institute for Immunology was founded and is supported by F. Hoffmann-La Roche Ltd., Basel, Switzerland.

Correspondence and requests for material should be addressed to A.G.R. (e-mail: rolink@bii.ch).

Dimerization inhibits the activity of receptor-like protein-tyrosine phosphatase-α

Guoqiang Jiang*, Jeroen den Hertog†, Jing Su§, Joseph Noel‡, Jan Sap§ & Tony Hunter*

** Molecular Biology and Virology Laboratory and ‡ Structural Biology Laboratory, The Salk Institute for Biological Studies, 10010 North Torrey Pines Rd, La Jolla, California 92037, USA*
† Hubrecht Laboratory, Netherlands Institute for Developmental Biology, Uppsalalaan 8, 3584 CT Utrecht, The Netherlands
§ New York University Medical Center, Department of Pharmacology, New York, New York 10016, USA

Protein-tyrosine phosphatases (PTPs) are vital for regulating tryosine phosphorylation in many processes, including growth and differentiation[1,2]. The regulation of receptor-like PTP (RPTP) activity remains poorly understood, but based on the crystal structure of RPTPα domain 1 we have proposed that dimerization can negatively regulate activity, through the interaction of an inhibitory 'wedge' on one monomer with the catalytic cleft of domain 1 in the other monomer[3,4]. Here we show that dimerization inhibits the activity of a full-length RPTP *in vivo*. We generated stable disulphide-bonded full-length RPTPα homodimers by expressing mutants with single cysteines at different positions in the ectodomain juxtamembrane region. Expression of wild-type RPTPα and Phe135Cys and Thr141Cys mutants in RPTPα-null mouse embryo cells increased dephosphorylation and activity of Tyr 529 in the protein tyrosine kinase c-Src; in contrast, expression of a Pro137Cys mutant did not. Mutation of Pro 210/211 to leucine in the inhibitory wedge of the Pro137Cys mutant restored its ability to activate c-Src, indicating that dimerization may inhibit full-length RPTPα activity in a manner stereochemically consistent with RPTPα crystal structures[3]. Our results suggest that RPTPα activity can in principle be negatively regulated by dimerization *in vivo*.

Of the ~75 PTP members identified so far, ~25 are RPTPs[2]. The mechanisms for regulating RPTP activity are mostly unknown, but emerging functional evidence indicates that homodimerization may inhibit CD45 RPTP activity[5–7], and heterodimerization inhibits RPTPσ (ref. 8). RPTPα has a typical RPTP structure with two cytoplasmic catalytic domains (Fig. 1a)[9], which are both active[10]. RPTPα associates with c-Src[11] and directly dephosphorylates the negative regulatory Tyr in c-Src (Tyr 529 in mouse c-Src), leading to its activation[12–15]. In two crystal forms, murine RPTPα-D1 exists as a symmetrical dimer, in which a wedge-shaped helix–turn–helix element on one monomer inserts into the active site of the dyad-related monomer, resulting in mutual active-site occlusion. This

indicated that RPTPα may be able to form dimers and that, if formed, these dimers would have decreased PTP activity[3].

To test this model, we generated covalently stabilized RPTPα dimers with an intermolecular disulphide bond by introducing single unpaired Cys at several positions in the extracellular domain in the region immediately adjacent to the transmembrane domain (TMD) (residues 143–166), as done for Neu/ErbB2 (refs 16, 17) and the epidermal growth factor (EGF) receptor[18]. To maximize the chances of obtaining disulphide-linked RPTPα dimers, we made four single Cys mutations (F135C, P137C, D139C and T141C) within a seven-residue span (residues 135–141), directly amino-terminal to the TMD (residues 143–166) of a haemagglutinin (HA)-tagged full-length (FL) RPTPα construct (Fig. 1a). As there are no other Cys in the RPTPα ectodomain, the free Cys should form an interchain disulphide bond between two RPTPα molecules if they can dimerize, thus stabilizing the dimer. Because TMDs are generally α-helical and are thought to emerge from the membrane in an α-helical conformation, these mutants would place a Cys at four different phases on the α-helical wheel, which repeats every seven residues. Dimers of the four Cys mutants should have the two intracellular catalytic domains in different relative rotational orientations, which could be important if a specific spatial relationship is necessary to bring about attenuation of PTP activity by dimerization, as is the case for Neu/ErbB2 activation[17].

The wild-type RPTPα and Cys-mutant proteins, which were overexpressed in HEK 293 cells by transient transfection, all

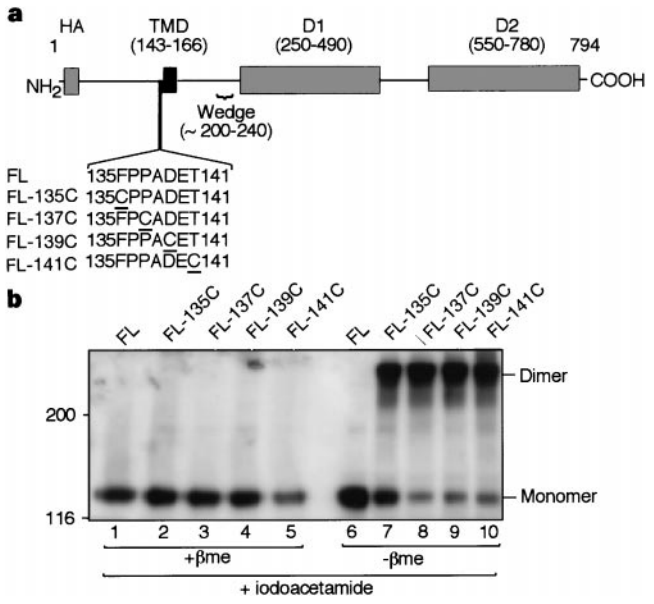

Figure 1 Dimerization of full-length RPTPα via intermolecular disulphide bonds. **a**, Diagram of HA-tagged full-length wild type (FL) RTPα and Cys mutants based on the original (untagged) polypeptide[9] and D1 crystal structure[3]. **b**, Reducing and nonreducing SDS–PAGE and immunoblotting (IB) analysis of the whole cell lysates of transiently transfected HEK 293 cells. + iodoacetamide, 20 mM iodoacetamide in lysis buffer; + or – βme, presence or absence of β-mercaptoethanol in the loading buffer. The positions of relative molecular mass markers (in thousands) are indicated on the left side of the gel. Similar abbreviations are used in all figures.

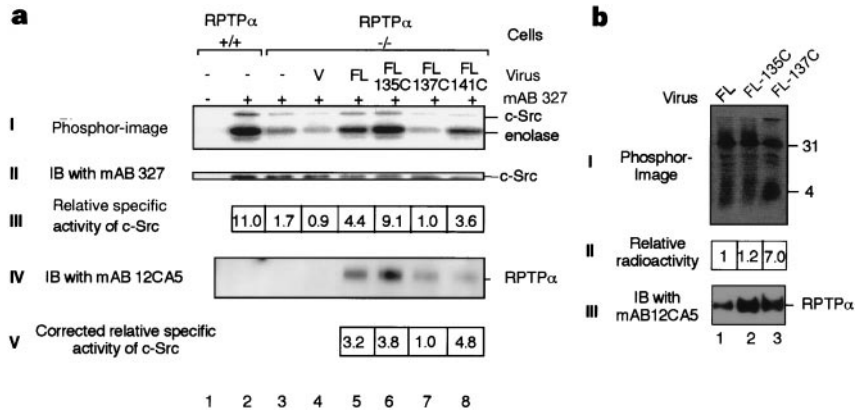

Figure 2 Mutant FL–137C has a much reduced ability to activate c-Src in RPTPα$^{-/-}$ cells. **a**, *In vitro* phosphorylation. RPTPα$^{+/+}$ cells and RPTPα$^{-/-}$ cells were either mock-infected (–), infected with control virus not encoding RPTPα (V) or infected with retrovirus expressing FL, FL-135C, FL-137C or FL-141C as indicated. Monoclonal antibody (mAB) 327 was used for c-Src immunoprecipitation from cell lysates (+) (lanes 2–8) but was omitted in the control (–) (lane 1). Panel I, Phosphorimage showing enolase phosphorylated by c-Src and autophosphorylated c-Src. Panel II, Immunoblot with mAB 327 showing the levels of c-Src in the immunoprecipitate (IPs). Panel III, The specific activity of c-Src was determined as the ratio of the level of phosphorylated enolase in panel I (quantified by phosphorimaging using ImageQuant software) to the level of c-Src in panel II (quantified by densitometry using NIH Image Version 1.57 software). Panel IV, Immunoblot of whole cell lysates with mAB 12CA5 showing the levels of exogenously expressed HA-tagged RPTPα. Panel V, Corrected relative specific activity of c-Src was determined by normalizing the relative c-Src specificity in panel III with RPTPα expression level in panel IV (quantified by densitometry using NIH Image Version 1.57 software). Similar results were observed in three experiments, and the results of a representative experiment are shown. **b**, Analysis of c-Src phosphorylation by CNBr phosphopeptide mapping performed four days after retroviral infection as described[12]. Panel I, Phosphorimage. Panel II, Quantification of the 4,000 M_R phosphorylated-Tyr529-containing phosphopeptide using ImageQuant software. Panel III, RPTPα in the ^{32}P-labelled lysate was immunoprecipitated and detected by IB using mAB 12CA5.

migrated at a relative molecular mass of ~130 K in SDS–polyacrylamide gel electrophoresis (PAGE) under reducing conditions, as determined by immunoblotting (Fig. 1b, lanes 1–5). In contrast, all of the Cys-mutant proteins, but not the wild-type protein, migrated predominantly at ~260 K under nonreducing conditions (Fig. 1b, lanes 6–10). This indicates that the RPTPα proteins were correctly expressed and fully glycosylated, and that the Cys mutants efficiently oligomerized *in vivo* through disulphide-bond formation. We confirmed that the RPTPα oligomers were actually homodimers because FL-135C and a truncated FL-135C mutant lacking the cytoplasmic domain formed heterodimers when coexpressed in 293 cells (data not shown).

We have been unable to assay the PTP activity of the Cys dimers *in vitro*, because the iodoacetamide included in the lysis buffer to prevent cleavage of the RPTPα dimers following cell lysis alkylates the active-site Cys and abrogates catalytic activity. In the absence of iodoacetamide, the proportion of dimeric RPTPα was significantly reduced because endogenous cellular glutathione reduces the disulphide bond and thus dissociates the dimer (data not shown). For this reason, we resorted to an *in vivo* assay for RPTPα activity, in which we determined the ability of retrovirally transduced wild-type and mutant RPTPα to dephosphorylate Tyr 529 of c-Src and thereby increase the activity of c-Src in RPTPα$^{-/-}$ fibroblasts derived from RPTPα knock-out mice[14]. RPTPα$^{-/-}$ cells have greatly reduced c-Src activity[14]. Four days after retroviral infection, when expression of RPTPα protein peaked (data not shown), infected RPTPα$^{-/-}$ cells were lysed (for technical reasons we have been unable to generate an FL-139C retrovirus). Endogenous c-Src protein was isolated by immunoprecipitation using anti-Src monoclonal antibody 327, and its activity was measured by *in vitro* phosphorylation experiments using enolase as a substrate. c-Src activity was clearly detectable in RPTPα$^{+/+}$ cells (Fig. 2a, I and II, lane 2), being ~40 fold higher than that in a control without monoclonal antibody 327 (compare lanes 1 and 2, quantification not shown). As shown previously[14], the specific activity of c-Src was ~6 fold lower in RPTPα$^{-/-}$ cells than in RPTPα$^{+/+}$ cells (Fig. 2a, I, II and III, lanes 2 and 3). Expression of the wild-type RPTPα (FL) significantly increased the specific activity of c-Src (lanes 4 and 5), as did the expression of FL-135C and FL-141C (Fig. 2a, lanes 4, 6 and 8). However, expression of FL-137C did not activate c-Src (lanes 4 and 7). Immunoblotting analysis showed that FL-137C was expressed to at least the same level as FL-141C (Fig. 2a, IV, lanes 7 and 8). In fact, FL-137C failed to activate c-Src, as well as the wild type, even when it was expressed at a higher level than the wild-type protein (see Fig. 4). When corrected for RPTPα expression levels, FL, FL-135C, and FL-141C proteins all activated c-Src to a similar extent, whereas FL-137C always activated c-Src more weakly (Fig. 2a, V, lanes 5, 6, 7 and 8). CNBr peptide mapping of *in vivo* ^{32}P-labelled c-Src indicates that c-Src Tyr 529 phosphorylation was higher in cells expressing FL-137C than in cells expressing FL or FL-135C, consistent with the lower Src activity in the FL-137C-expressing cells (Fig. 2b). Similar results were obtained from multiple experiments.

Immunofluorescence confocal microscopy showed indistinguishable plasma membrane staining for RPTPα in cells expressing either FL (Fig. 3b) or FL-137C (Fig. 3c), whereas plasma membrane staining was not detected in the cells infected with control retrovirus (Fig. 3a). Cell-surface labelling by biotinylation followed by immunoprecipitation of RPTPα showed that FL and FL-137C were localized to the cell surface in proportion to their expression levels (Fig. 3d, lanes 1 and 2). We therefore conclude that FL-137C was correctly localized to the plasma membrane. Together, these results indicate that dimerization through Cys at position 137, but not at position 135 or position 141, reduces the ability of RPTPα to dephosphorylate Try 529 in c-Src. Our results also indicate that an inhibited dimer may only form when the monomers in the dimer are oriented in a particular geometry with respect to one another. In other words, to be functionally inhibited, the PTP dimer may require a specific rotational coupling, as is the case for activation of Neu/ErbB2 by Cys-induced dimerization[17]. By chemical cross-linking, we have obtained evidence that full-length RPTPα homodimerizes extensively on the cell surface (G.J., J.d.H. and T.H., unpublished observations). However, RPTPα exists on the cell surface as populations of monomers and dimers in equilibrium,

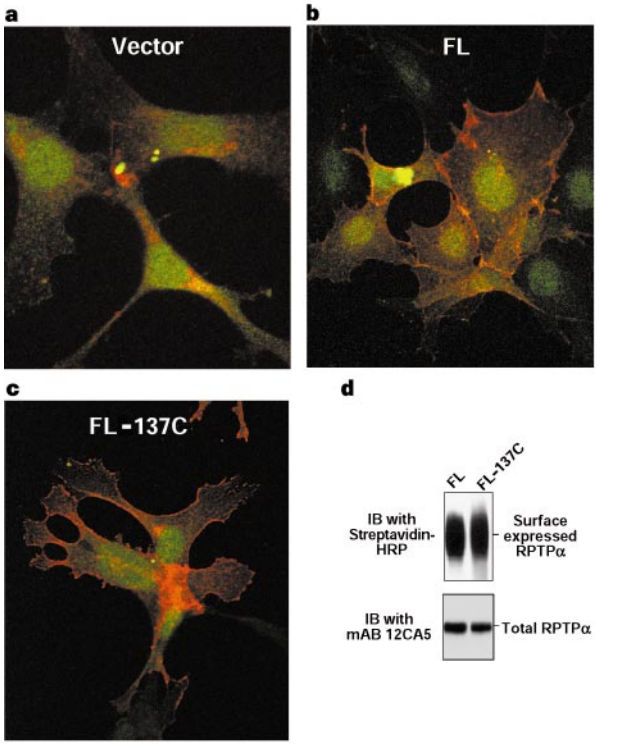

Figure 3 Membrane localization of RPTPα proteins. Immunofluorescence staining of RPTPα$^{-/-}$ cells infected with control retrovirus (**a**), retrovirus expressing FL (**b**) or FL-137C (**c**) was performed as described[23] using mAB 12CA5 and goat anti-mouse Ig-Texas Red (1:200 dilution; Southern Biotechnology, Inc.). Confocal microscopy images are shown. Red fluorescence, HA-tagged RPTPα. Green fluorescence, GFP. **d**, Cell-surface biotinylation of intact transiently transfected 293 cells was performed as described[28] using EZ-link-Sulfo-NHS-LC-Biotin (Pierce). FL and FL-137C proteins were immunoprecipitated with antiserum 5478 and detected by IB with either Streptavidin-HRP for surface-expressed RPTPα (top) or mAB 12CA5 for total RPTPα (bottom).

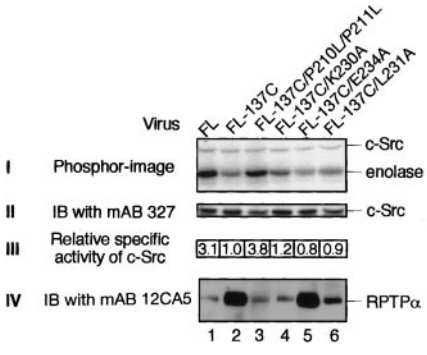

Figure 4 A P210/P211L double mutation in the wedge region activates RPTPα FL-137C. RPTPα$^{-/-}$ cells were infected with retrovirus expressing either FL, FL-137C, FL-137C/P210L/P211L, FL-137C/K230A, FL-137C/E234A, or FL-137C/L231A RPTPα, and the relative specific activity of the c-Src in mAB 327 IPs was measured by *in vitro* phosphorylation using enolase as a substrate as described in Fig. 2. Similar results were observed in three experiments and the results of a representative experiment are shown.

and the inhibition by Cys 137-mediated dimerization therefore occurs by locking RPTPα into the inactive dimeric state.

To test whether the wedge-mediated interactions predicted by the RPTPα D1 crystal structure are needed for the loss of activity in the FL-137C dimer, we investigated the effect of wedge mutations on the activity of the FL-137C mutant protein. Mutations in the wedge region were made in FL-137C by substituting Pro 210/211 with Leu, and Lys 230, Glu 234 and Leu 231 individually with Ala. Pro 210 and 211 are in the elbow of the wedge and play an important role in holding the wedge rigid, and Lys 230 and Glu 234 make direct contacts with residues in the active site, whereas Leu 231, mutated as a control, does not appear to be involved in dimerization[3]. Expression of FL-137C/P210L/P211L led to activation of c-Src to a similar extent as FL RPTPα (Fig. 4, I, II and III, lanes 1 and 3), whereas expression of FL-137C, FL-137C/K230A, FL-137C/E234A and FL-137C/L231A did not activate c-Src (Fig. 4, I, II and III, lanes 2, 4, 5 and 6), even when expressed at much higher levels than the FL and FL-137C/P210L/P211L proteins (Fig. 4, IV, lanes 1, 2, 3, 5 and 6). Similar results were obtained in repeated experiments (the wedge mutants were typically expressed at lower levels than FL-137C; in Fig. 4, the expression of FL wild-type protein was atypically low, but this experiment was chosen because its level is equal to that of FL-137C/P210L/P211L). Consistent with the *in vitro* phosphorylation experiments, immunoblotting analysis using monoclonal antibody clone 28 (ref. 19), which recognizes the activated form of c-Src containing unphosphorylated Tyr 529, showed that c-Src Tyr 529 phosphorylation was lower in cells expressing FL or FL-137C/P210L/P211L than in cells expressing FL-137C and other wedge mutants (data not shown). Cell-surface labelling by biotinylation showed that all the wedge mutants were localized to the cell surface in proportion to their expression levels, as with FL and FL-137C (data not shown). This indicates that the P210/211L double mutations, but not the single mutations in the wedge region, significantly restored the activity of FL-137C. Consistent with the c-Src activity assay, chemical crosslinking experiments showed that P210/P211L double mutation reduced the dimerization efficiency of RPTPα compared with wild type (G.J., J.d.H. and T.H., unpublished observations).

In summary, our evidence indicates that RPTPα can dimerize *in vivo*, and that dimerization decreases the catalytic activity of full-length RPTPα *in vivo* through a wedge region interaction, as proposed[3]. This is also in keeping with results from the EGFR–CD45 dimer[6]. As other RPTPs have the potential to dimerize[7,20], dimerization may represent a physiologically relevant negative regulatory mechanism for a subset of RPTPs as proposed[3,4]; however, there is structural evidence that other RPTPs may not be regulated by dimerization[21,22]. The mechanism by which RPTPα dimerization might be regulated remains to be elucidated. Phosphorylation of Ser 180/204 in the juxtamembrane region by protein kinase C, which enhances activity, is one possible mechanism[23,24]. Alternatively, a ligand that induces dimerization of RPTPα or stabilizes the monomeric state may exist. □

Methods

Expression vectors, site-directed mutagenesis and antibodies

The complementary DNA encoding a full length murine RPTPα (FL) with an HA epitope inserted between amino acids 19 and 20 has been described[25]. Cys mutants FL-135C, FL-137C, FL-139C and FL-141C (Fig. 1a) were prepared using the Quikchange Site-Directed Mutagenesis Kit (Stratagene) with sense mutagenesis primers: 135C Top (5′-ccactccagaaacctggcccccggcag-3′); 137C Top (5′-ccagaaaccttcccctgtgcagatgagacacc-3′); 139C Top (5′-ccccccggcatgtgagacaccaattattgc-3′); and 141C Top (5′-cccggcagatgagtgtccaattattgcgg-3′). Wedge mutants in the P137C background were also prepared by mutagenesis using the following sense primers: P210/211L (5′-aggaagtacctactactgcctgtg-3′); D227A (5′-agaatggctgctgacaataag-3′); K230A (5′-gatgacaatgcgatcttcaga-3′); E234A (5′-ctcttcagag-cagaattcaac-3′); and L231A (5′-gacaataaggccttcagagaa-3′). The cDNAs were cloned into both the mammalian expression vector pSG5 (ref. 25) and the retroviral expression vector pCR2. pCR2 is a bicistronic vector based on the pCL series[26] (C.A. Joazeiro, unpublished data), and the recombinant vector expresses green fluorescent protein (GFP) and RPTPα simultaneously. 12CA5 is a mouse monoclonal antibody against the HA epitope; 5478 is a rabbit polyclonal antiserum raised against a glutathione-*S*-transferase (GST)-fusion protein containing the entire cytoplasmic domain of murine RPTPα (ref. 23); 327 is a mouse monoclonal antibody raised against v-Src that also recognizes c-Src[27].

Cells, transient transfections, retrovirus packaging and infections

RPTPα$^{-/-}$ cells and RPTPα$^{+/+}$ cells are embryonic fibroblasts derived from RPTPα knock-out mice and normal (control) mice, respectively[14]. These and HEK 293 cells were cultured in Dulbecco's-modified Eagle's medium supplemented with 10% fetal bovine serum at 37 °C and 10% CO_2. Transient transfection of 293 cells was done by calcium phosphate precipitation[12]. For protein expression, cells were harvested 48 h after transfection. For retrovirus production, 15 μg recombinant retrovirus vector and 10 μg ecotropic packaging vector pCL.ECO[26] were co-transfected into 293 cells. Media containing retrovirus were harvested at 36, 48 and 60 h by replenishing 3 ml of fresh medium after each harvest, and the virus-containing media were pooled and filtered. For infection, RPTPα$^{-/-}$ cells were seeded onto 50-mm tissue-culture dishes 24 h before infection with the virus-containing media containing 5 μg ml^{-1} polybrene every 12 h, a total of three times. Generally, nearly 100% of the cells were GFP positive and infected, as judged by fluorescence-activated cell sorting analysis (data not shown).

Immunoprecipitation and *in vitro* phosphorylation

RPTPα$^{-/-}$ cells were seeded onto 50-mm plates and infected with retrovirus as described above. RPTP$^{+/+}$ cells, when used, were exposed to polybrene but not to retrovirus. Cells were lysed in 0.75 ml RIPA buffer[23]. The levels of exogenously overexpressed RPTPα were determined by immunoblotting whole cell lysates using monoclonal antibody 12CA5. The c-Src was immunoisolated with anti-Src monoclonal antibody 327 and its activity was assayed by *in vitro* phosphorylation experiments using enolase as substrate as described[12]. The levels of c-Src in the immunoprecipitates were determined by immunoblotting using monoclonal antibody 327.

Received 5 July; accepted 26 August 1999.

1. Hunter, T. Protein kinases and phosphatases: the yin and yang of protein phosphorylation and signaling. *Cell* **80,** 225–236 (1995).
2. Tonks, N. K. & Neel, B. G. From form to function: signaling by protein tyrosine phosphatases. *Cell* **87,** 365–368 (1996).
3. Bilwes, A. M., den Hertog, J., Hunter, T. & Noel, J. P. Structural basis for inhibition of receptor protein-tyrosine phosphatase α by dimerization. *Nature* **382,** 555–559 (1996).
4. Weiss, A. & Schlessinger, J. Switching signals on or off by receptor dimerization. *Cell* **94,** 277–280 (1998).
5. Desai, D. M., Sap, J., Schlessinger, J. & Weiss, A. Ligand-mediated negative regulation of a chimeric transmembrane receptor tyrosine phosphatase. *Cell* **73,** 541–554 (1993).
6. Majeti, R., Bilwes, A. M., Noel, J. P., Hunter, T. & Weiss, A. Dimerization-induced inhibition of receptor protein tyrosine phosphatase function through an inhibitory wedge. *Science* **279,** 88–91 (1998).
7. Felberg, J. & Johnson, P. Characterization of recombinant CD45 cytoplasmic domain proteins. Evidence for intramolecular and intermolecular interactions. *J. Biol. Chem.* **273,** 17839–17845 (1998).
8. Wallace, M. J., Fladd, C., Batt, J. & Rotin, D. The second catalytic domain of protein tyrosine phosphatase δ (PTPδ) binds to and inhibits the first catalytic domain of PTPσ. *Mol. Cell. Biol.* **18,** 2608–2616 (1998).
9. Sap, J., D'Eustachio, P., Givol, D. & Schlessinger, J. Cloning and expression of a widely expressed receptor tyrosine phosphatase. *Proc. Natl Acad. Sci. USA* **87,** 6112–6116 (1990).
10. Wu, L., Buist, A., den Hertog, J. & Zhang, Z. Y. Comparative kinetic analysis and substrate specificity of the tandem catalytic domains of the receptor-like protein-tyrosine phosphatase α. *J. Biol. Chem.* **272,** 6994–7002 (1997).
11. Harder, K. W., Moller, N. P., Peacock, J. W. & Jirik, F. R. Protein-tyrosine phosphatase α regulates Src family kinases and alters cell-substratum adhesion. *J. Biol. Chem.* **273,** 31890–31900 (1998).
12. den Hertog, J. *et al.* Receptor protein tyrosine phosphatase α activates pp60$^{c\text{-}src}$ and is involved in neuronal differentiation. *EMBO J.* **12,** 3789–3798 (1993).
13. Zheng, X. M., Wang, Y. & Pallen, C. J. Cell transformation and activation of pp60$^{c\text{-}src}$ by overexpression of a protein tyrosine phosphatase. *Nature* **359,** 336–339 (1992).
14. Su, J., Muranjan, M. & Sap, J. Receptor protein tyrosine phosphatase α activates Src-family kinases and controls integrin-mediated responses in fibroblasts. *Curr. Biol.* **9,** 505–511 (1999).
15. Ponniah, S., Wang, D. Z., Lim, K. L. & Pallen, C. J. Targeted disruption of the tyrosine phosphatase PTPα leads to constitutive downregulation of the kinases Src and Fyn. *Curr. Biol.* **9,** 535–538 (1999).
16. Cao, H., Bangalore, L., Dompe, C., Bormann, B. J. & Stern, D. F. An extra cysteine proximal to the transmembrane domain induces differential cross-linking of p185^{neu} and p185^{neu*}. *J. Biol. Chem.* **267,** 20489–20492 (1992).
17. Burke, C. L. & Stern, D. F. Activation of Neu (ErbB-2) mediated by disulfide bond-induced dimerization reveals a receptor tyrosine kinase dimer interface. *Mol. Cell. Biol.* **18,** 5371–5379 (1998).
18. Sorokin, A., Lemmon, M. A., Ullrich, A. & Schlessinger, J. Stabilization of an active dimeric form of the epidermal growth factor receptor by introduction of an inter-receptor disulfide bond. *J. Biol. Chem.* **269,** 9752–9759 (1994).
19. Kawakatsu, H. *et al.* A new monoclonal antibody which selectively recognizes the active form of Src tyrosine kinase. *J. Biol. Chem.* **271,** 5680–5685 (1996).
20. Takeda, A., Wu, J. J. & Maizel, A. L. Evidence for monomeric and dimeric forms of CD45 associated with a 30-kDa phosphorylated protein. *J. Biol. Chem.* **267,** 16651–16659 (1992).
21. Hoffmann, K. M., Tonks, N. K. & Barford, D. The crystal structure of domain 1 of receptor protein-tyrosine phosphatase μ. *J. Biol. Chem.* **272,** 27505–27508 (1997).
22. Nam, H. J., Poy, F., Krueger, N. X., Saito, H. & Frederick, C. A. Crystal structure of the tandem phosphatase domains of RPTP LAR. *Cell* **97,** 449–457 (1999).
23. Tracy, S., van der Geer, P. & Hunter, T. The receptor-like protein-tyrosine phosphatase, RPTP α, is phosphorylated by protein kinase C on two serines close to the inner face of the plasma membrane. *J. Biol. Chem.* **270,** 10587–10594 (1995).

24. den Hertog, J., Sap, J., Pals, C. E., Schlessinger, J. & Kruijer, W. Stimulation of receptor protein-tyrosine phosphatase α activity and phosphorylation by phorbol ester. *Cell. Growth Differ.* **6,** 303–307 (1995).
25. den Hertog, J. & Hunter, T. Tight association of GRB2 with receptor protein-tyrosine phosphatase α is mediated by the SH2 and C-terminal SH3 domains. *EMBO J.* **15,** 3016–3027 (1996).
26. Naviaux, R. K., Costanzi, E., Haas, M. & Verma, I. M. The pCL vector system: rapid production of helper-free, high-titer, recombinant retroviruses. *J. Virol.* **70,** 5701–5705 (1996).
27. Lipsich, L. A., Lewis, A. J. & Brugge, J. S. Isolation of monoclonal antibodies that recognize the transforming proteins of avian sarcoma viruses. *J. Virol.* **48,** 352–360 (1983).
28. Levy-Toledano, R., Caro, L. H., Hindman, N. & Taylor, S. I. Streptavidin blotting: a sensitive technique to study cell surface proteins; application to investigate autophosphorylation and endocytosis of biotin-labeled insulin receptors. *Endocrinology* **133,** 1803–1808 (1993).

Acknowledgements

We are grateful to C. Joazeiro for providing the pCR2 retroviral vector and to W. Eckhart and P. Blume-Jensen for suggestions and critical review of the manuscript. This work is supported by grants from the National Cancer Institute (T.H.) and Dutch Cancer Society (J.d.H.). T.H. is a Frank and Else Schilling American Cancer Society Research Professor. G.J. is supported by a fellowship from the American Cancer Society.

Correspondence and requests for materials should be addressed to G.J. (e-mail: gjiang@aim.salk.edu).

Phytochrome signalling is mediated through nucleoside diphosphate kinase 2

Giltsu Choi*, Hankuil Yi*, Jaeho Lee†, Yong-Kook Kwon‡, Moon Soo Soh*, Byongchul Shin*, Zigmund Luka*, Tae-Ryong Hahn† & Pill-Soon Song*‡§

* *Kumho Life and Environmental Science Laboratory, Kwangju 500-712, Korea*
† *Department of Genetic Engineering, Kyung Hee University, Suwon 449-701, Korea*
‡ *Department of Chemistry, University of Nebraska, Lincoln, Nebraska 68588, USA*
§ *Department of Life Science, Kwangju Institute of Science and Technology, Kwangju 500-712, Korea*

Because plants are sessile, they have developed intricate strategies to adapt to changing environmental variables, including light. Their growth and development, from germination to flowering, is critically influenced by light, particularly at red (660 nm) and far-red (730 nm) wavelengths[1,2]. Higher plants perceive red and far-red light by means of specific light sensors called phytochromes(A–E)[3]. However, very little is known about how light signals are transduced to elicit responses in plants. Here we report that nucleoside diphosphate kinase 2 (NDPK2) is an upstream component in the phytochrome signalling pathway in the plant *Arabidopsis thaliana*. In animal and human cells, NDPK acts as a tumour suppressor[4]. We show that recombinant NDPK2 in *Arabidopsis* preferentially binds to the red-light-activated form of phytochrome *in vitro* and that this interaction increases the activity of recombinant NDPK2. Furthermore, a mutant lacking NDPK2 showed a partial defect in responses to both red and far-red light, including cotyledon opening and greening. These results indicate that NDPK2 is a positive signalling component of the phytochrome-mediated light-signal-transduction pathway in *Arabidopsis*.

Biochemical approaches have identified the heterotrimeric guanine-nucleotide-binding protein Ca^{2+}/CaM and cyclic GMP as components of phytochrome-mediated light-signal-transduction pathways[3]. Indeed, the phosphorylation and dephosphorylation of specific proteins, including phytochrome, may be involved[5,6]. Genetic approaches have identified ten pleiotropic mutants (*cop/fus/det*) that display constitutively photomorphogenic phenotypes and several other photomorphogenic mutants[7]; some mutants specific to a certain phytochrome signal-transduction pathway have also been identified[8–13]. However, the recently identified PIF3 and PKS1 are the only signalling components that interact directly with phytochrome to have been thoroughly investigated[14,15].

We used a yeast two-hybrid screening method to identify proteins associated with phytochrome A. As the bait, we used the carboxy-terminal domain of *Arabidopsis* phytochrome A (position 568–1193). From the screening, we identified 52 yeast colonies that expressed both reporter genes (*his3*$^+$/*lacZ*$^+$) in a phytochrome-A-dependent manner, three of which encoded phytochrome A (two clones, position 588–1193; one clone, position 943–1193) (data not shown). Identification of the expected phytochrome A clones from the screening indicated that the C-terminal domain of phytochrome A has the correct folding structure in yeast, so it can be used to identify other phytochrome-associated proteins.

Sequence analysis indicated that 26 phytochrome-A-associated proteins are NDPK2. NDPK2 interacted specifically with phytochrome A, but not with DNA-binding domain of GAL4 alone or those fused to other proteins such as laminin C and p53 (Fig. 1a).

We established whether two spectral forms of phytochrome interact differently with NDPK2 by using purified recombinant *Arabidopsis* NDPK2 and oat phytochrome (Fig. 1b). Recombinant

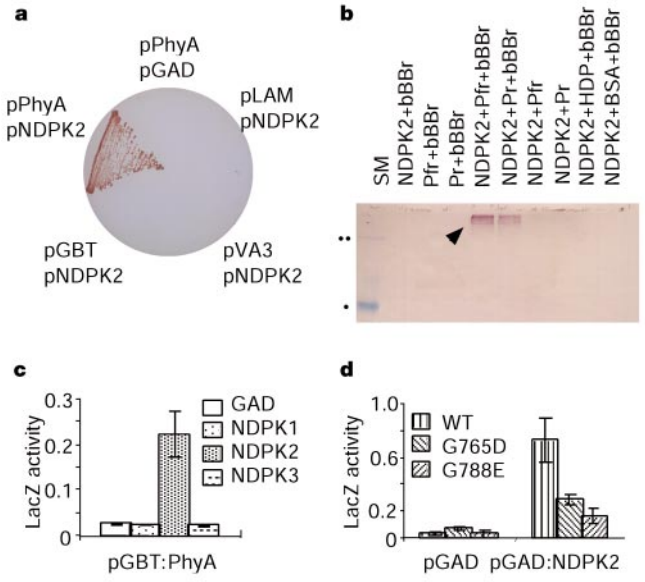

Figure 1 NDPK2 interacts preferentially with the P_{fr} form of phytochrome, whereas NDPK1 and NDPK3 do not interact. **a**, Specific interaction between NDPK2 and phytochrome A. pPhyA, position 568–1193 of *Arabidopsis* phytochrome A in pGBT9; pLAM and pVA3, laminin and p53 in pGBT9; pNDPK2, the full-length NDPK2 in pGAD424; pGBT, pGBT9. Yeasts were plated on HIS-dropout plates. **b**, *In vitro* crosslinking assay between NDPK2 and phytochrome. Arrow indicates crosslinked products of high relative molecular mass; 250 K (two dots) and 98 K (one dot) size markers (SM) are indicated. NDPK2, recombinant NDPK2; bBBr, the crosslinking agent bisbromobimane; Pfr and Pr, different spectral forms (P_{fr} and P_r) of phytochrome; HDP, heat-denatured phytochrome; BSA, bovine serum albumin. **c**, ONPG assay showing that only NDPK2 interacts with phytochrome A. Genes encoding NDPK were in pGAD424 vectors (NDPK1, NDPK2 and NDPK3). GAD, a control vector containing only the GAL4 activation domain. Position 656–1193 of wild-type phytochrome A (pGBT:PhyA) was used as bait. LacZ activity was expressed as the ratio of absorbance at 420 and 600 nm. Error bar, standard deviation. **d**, ONPG assay showing that two identified missense mutations in phytochrome A disrupt the interaction with NDPK2 (pGAD:NDPK2). Position 656–1193 of wild-type (WT) and mutant (G765D, G788E) phytochrome A in pGBT9 was used. Error bar, standard deviation.